Title
Directional polarization sensitivity of articular cartilage by optical coherence tomography

Authors
Xie, Tuqiang
Guo, Shouguang
Zhang, Jun
et al.

Publication Date
2006-02-09

DOI
10.1117/12.649112

Directional polarization sensitivity of articular cartilage by optical coherence tomography

Tuqiang Xie, Shouguang Guo, Jun Zhang, Zhongping Chen and George M. Peavy
Beckman Laser Institute, University of California, Irvine
1002 Health Sciences Road East, Irvine, CA 92612

Abstract

In this paper, the polarization sensitivity of articular cartilage was investigated by using polarization sensitivity optical coherence tomography (PS-OCT) obtained by varying the angel of incident illumination. Experimental results show that when the incident light is perpendicular to the tissue surface, normal articular cartilage demonstrates little polarization sensitivity. Significant variations in birefringence of articular cartilage observed when the angle of incident light was adjusted between 0º and 90º relative to the tissue surface. Directional polarization sensitivity of articular cartilage as obtained by PS-OCT imaging using variations in the angle of incident illumination can be used to access the orientation and organization of the collagen matrix of these tissues. The polarization sensitivity and the birefringence images obtained can be explained by the angle of illumination relative to the unique microstructure and orientation of the collagen fibrils and fibers of articular cartilage.

Keywords: optical coherence tomography, medical optics instrumentation, medical and biological imaging, polarization-sensitive device; birefringence.

1. Introduction

Degenerative joint disease (DJD) or asteoarthritis can be a severely debilitating disease and is the second most common cause of working disability only to heart disease [1]. To evaluate treatment effects and develop appropriate and efficacious treatment strategies, it is important to understand this disease and to be able to accurately access the collagen microstructure of cartilage and monitor in vivo the progression of disease or response to treatment. Diagnostic biopsy of articular cartilage is not advised because of its limited regenerative capacity, and conventional morphological imaging methods including radiographs, computed tomography (CT), ultrasound and magnetic resonance imaging (MRI) have been applied to the diagnosis of cartilage abnormalities [2, 3, 4, 5]. However, these methods provide insufficient resolution for evaluation of micro-structural changes.

As a new morphological imaging technique, optical coherence tomography (OCT) allows non-invasive high-resolution cross-sectional imaging of tissue microstructure [6] and is adaptable to arthroscopy [7]. Conventional OCT is based on the intensity of backscattered optical radiation. Polarization-sensitive OCT (PS-OCT) also provides information on the polarization states of backscattered light, revealing properties of collagen matrix organization and integrity, not available by conventional OCT [8, 9]. Birefringence exists in many biological components such as collagen, retinal tissue, keratin, and myelin, and polarization properties of these biological components may be altered by injury or disease. PS-OCT has been used to study the microstructure and birefringence properties of biological tissues including skin, articular cartilage and intervertebral disc [10, 11, 12, 13]. Based on experimental results from polarization microscopy, normal cartilage is sensitive to the polarization of incident light and this polarization sensitivity (birefringence) is related to the organization of the collagen fibrils of the cartilage matrix. Because of this tissue birefringence, PS-OCT has been reported as a diagnostic tool for the assessment of matrix changes in degenerative joint disease (DJD) [11, 12].

Our recent experimental results have demonstrated that normal articular cartilage and DJD without matrix disorganization demonstrate little polarization sensitivity when PS-OCT images are obtained by scanning the specimens with the incident illumination normal (90º) to the specimen surface [12]. Polarization microscopy is performed on histological section of tissue in a transmission mode while PS-OCT is done in a reflection or backscattering mode on intact tissues from the tissue surface. While each technology may be used to evaluate tissue birefringence, the incident illumination to the tissue architecture differs between the imaging modes by 90º. Therefore, the tissue birefringence imaged by each method is determined in planes that are 90º different in orientation to the matrix organization. In this study, the directional polarization sensitivity of bovine articular cartilage was evaluated by a PS-OCT system to

Coherence Domain Optical Methods and Optical Coherence Tomography in Biomedicine X
edited by Valery V. Tuchin, Joseph A. Izatt, James G. Fujimoto, Proc. of SPIE Vol. 6079
60792E, (2006) · 1605-7422/06/$15 · doi: 10.1117/12.649112

investigate the relationship between the incident angle of illumination with respect to the collagen fiber orientation of the tissue matrix and the degree of birefringence observed.

2. Materials and Methods

The schematic diagram of PS-OCT setup is shown in Fig. 1 and has been described [12]. Unpolarized low coherence light from a superluminescent diode (SLD) with 10 mW output power, and a central wavelength of 1310 nm with a half-maximum-full-width (HMFW) spectral bandwidth of 80 nm was coupled into a 2×2 fiber optic non-polarizing coupler which split the light into reference and sample arms. In the reference arm, a four-step driving function is applied to the polarization modulator (Newport Co. USA), and each step introduces a $\pi/4$ phase shift. Since only vertical linearly polarized light can pass through the phase modulator, four different reference polarization states are selected, each separated by 45° angles over a great circle on a Poincare sphere. An electro-optic phase modulator (Sumitomo Osaka Cement Co. Ltd, Japan) was inserted in reference arm to generate a stable carrier frequency at 500 kHz for heterodyne detection. In the sample arm, backscattered light from the sample was combined with light of each of the four corresponding polarization states reflected from the reference arm. After recombination in the detector arm, the interfered beams were split into its horizontal and vertical components by a polarization beam splitter and detected by two photo-detectors (Laser Components, Inc.), then high pass filtered, amplified and digitalized and further processed by a computer.

The four corresponding polarization states scattered from the sample arm are obtained by phased-resolved processing of the interference fringe signals obtained from two perpendicular polarization detection channels. By measuring the envelop of the interferometer signal in two channels of orthogonal polarization and their phase difference, the corresponding Strokes vectors could be obtained and the optical phase retardation was calculated as a function of depth from normalized Stokes vectors [15, 16]. The axial resolution (Δz) of the OCT system is determined by the coherence length of the light source and $\Delta z = (2\ln 2/\pi)\cdot(\bar{\lambda}^2/\Delta\lambda)$ which is 10 μm for this system. The lateral or transverse resolution is determined by the focused spot size in analogy with conventional microscopy and is around 10 μm.

Articular cartilage is composed of several distinct morphological zones including the superficial zone, the middle zone, the deep zone and the calcified zone, with different compositional and matrix organizational characteristics and illustrated in Fig. 2 [17, 18, 19, 20]. There are two major components of articular cartilage: 1) a fluid phase containing proteoglycans and water, and 2) a solid matrix containing collagen (predominantly type II in articular cartilage). The collagen matrix contributes most to tensile behavior and integrity of cartilage tissue. Proteoglycans are large biomolecules that consist of a protein core with glycosaminoglycan side chains and constrained within the collagen matrix. Birefringence in cartilage is due to the asymmetrical collagen fibril structure and may change with derangement and mechanical failure in the collagen network while loss of proteoglycans and the breakdown of the cartilage collagen network are typical of DJD. Our recent experimental results have demonstrated that the phase retardation measured by PS-OCT is not altered by changes in proteoglycan content of articular cartilage [12], therefore the degree of birefringence of cartilage as determined by PS-OCT imaging is predominantly influenced by collagen fibril orientation and organization.

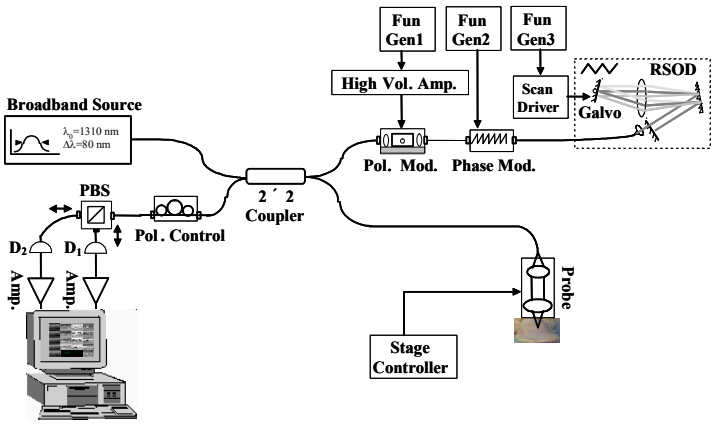

Fig. 1. Schematic diagram of PS-OCT system setup.

Fresh bovine articular cartilage specimens were collected from the rear legs of adult (5-7 year old) Holstein dairy cows slaughtered within the prior 36 hours. Full thickness samples that included subchondral bone were obtained for study from femoral-tibial joints by punch biopsy using a 1.0 cm diameter circular punch and mallet. A #11 scalpel blade was used to make 2 V-shaped marks on the edge of the cartilage specimen across the center from each other and the laser beam was scanned between these marks to obtain the specimen image. Each prepared specimen was wrapped in a 0.9% saline soaked gauze sponge, placed in a sealed and marked plastic bag, and held at room temperature until imaged on the same day. At the time of imaging, each specimen was removed from its protective wrapping, the base set in a 2 cm x 2 cm piece of paraffin for positioning and stabilization during imaging, and then placed in a 2 cm round disposable plastic Petri dish. The Petri dish was set on a rotation platform (PRM, Thorlabs, USA) by which three dimensional and angular adjustments could be made, and this was positioned under the controlled motorized sample arm of the imaging system so that the scanning beam, as evidenced by illumination from a superimposed 670 nm aiming beam, was passed across the surface of the cartilage specimen between the two V-shaped marks. The incident light from the focus lens of the sample arm is normally scanning across the surface of specimen at an angle normal (90º) to the surface as shown in Fig. 3 (A). In this study, the incident light beam was adjusted so that the specimen was illuminated at different angles (α) (Fig. 3(B)) away from the normal to the surface, and PS-OCT images were obtained with each variation of the angle of incident light. The specimens were orientated with an angle of 0° (normal incident to surface), 75° from the normalized direction to the surface of specimens, and 90° where the light was incident to the vertical cut of the specimen.

After OCT imaging, each specimen was fixed in 10% buffered formalin. Following tissue fixation each specimen was decalcified by being placed into 8% formic acid and checked daily until soft enough to section. Samples were then dehydrated in progressive concentrations of ethanol-water, cleared with Histoclear (National Diagnostics, Manville, NJ), and infiltrated with paraffin in an ATP1 tissue processor. The samples were then embedded in paraffin, cut perpendicularly to the articular cartilage surface in 6 μm thick serial sections made along the length of each specimen at its center where the OCT images had been obtained, and carefully placed on clean glass slides. The sections were deparaffinized with Histoclear, stained in Hematoxylin and Eosin-y (H&E) and coverslipped. The histology slides were imaged using a microscope (Nikon Microphot-fxa, Japan) with a real-time digital color microscope imaging camera (Microfire C, Optronics, CA, USA) coupled to a computer and recorded using image capture software (PictureFrame, ImagingPlanet, CA, USA).

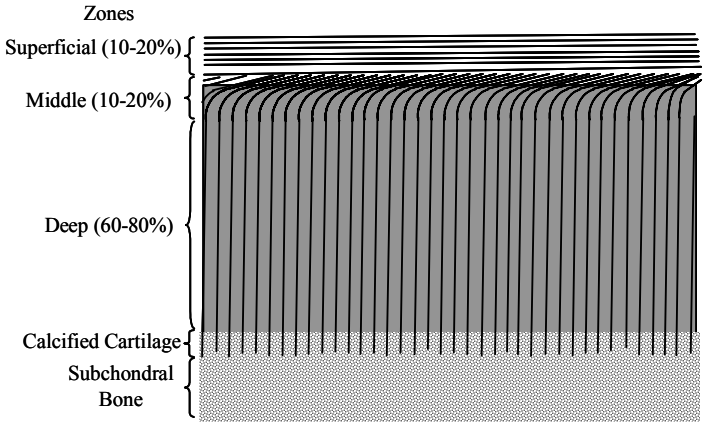

Fig. 2. Diagram of cartilage composition and architectural organization of the collagen matrix.

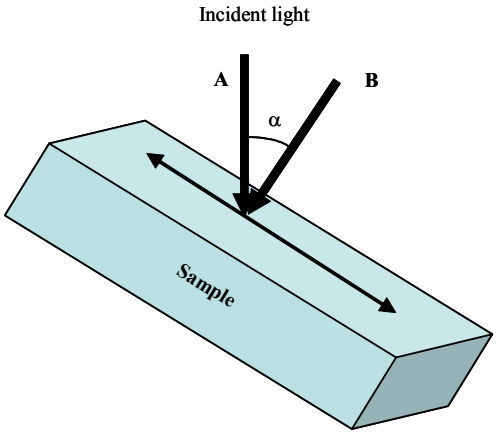

Fig. 3. Scanning light beam with an angle of 0º (A) or α (B).

3. Results

A normal bovine articular cartilage specimen was imaged by the PS-OCT system with the incident illumination adjusted to various angles ranging from being perpendicular to being parallel to the surface of the specimen. The surface images as viewed through a dissecting microscope from the two directions are shown in Fig. 4 (a) and (b). The OCT and Strokes vectors images and phase retardation images and histology are shown in Fig. 5 (a-g). The OCT image in Fig. 5 (a) had a high correlation with histology in Fig. 5 (g). It was found that normal bovine articular cartilage has little polarization sensitivity in Fig. 5 (b and c) when the scanning light from the sample arm is incident to the surface of the specimen at a right angle. In contrast, when the scanning light is incident to the deep zone of the specimen along a lateral cut surface at a direction parallel to the articular surface, the banded structure in the Strokes vectors images of Fig. 5 (e) clearly demonstrate that the tissue has strong polarization sensitivity, and the phase retardation image in Fig. 5(f) shows distinct retardation bands. The phase retardation of the tissue in relation to depth for the two different incident directions in normal articular cartilage is shown in Fig. 6. Since the cumulative phase retardation $\delta(z)$ is determined by the relationship $\delta(z) = \frac{2\pi}{\lambda_0}\Delta n \cdot z$, the degree of birefringence $\Delta n = n_e - n_o$ could be evaluated by the phase retardation slope in the phase retardation $\delta(z)$ versus depth (z), where n_e and n_o are the refractive indices for the ordinary ray and the extraordinary ray, respectively. The graphs of phase retardation versus depth in Fig. 6 show that normal bovine articular cartilage has little birefringence when the incident direction is perpendicular to articular surface but strong birefringence when the incident direction is parallel to the articular surface but perpendicular to the collagen matrix orientation of the deep zone.

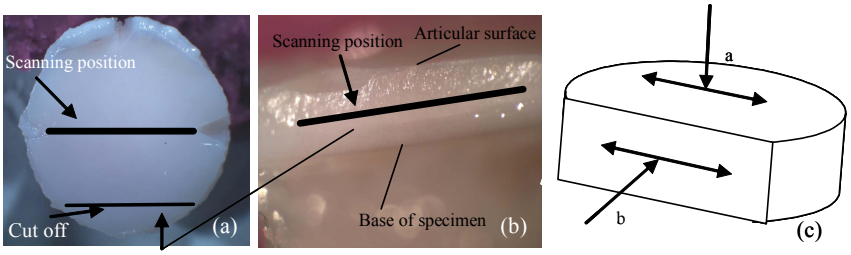

Fig. 4. Digital images of a normal articular cartilage specimen viewed through a dissecting microscope with the plane of view perpendicular (a) and parallel (b) to the specimen surface as illustrated (c).The view (b) was made along a lateral cut surface of the specimen.

To further investigate the directional polarization sensitive of the two kinds of tissues, PS-OCT images were obtained using different scanning angles relative to the articular surfaces and their Strokes vectors images were taken. The Strokes vectors and phase retardation images of normal articular cartilage are shown in Fig. 7(a-j) when the incident

light beam is 0°, 20°, 40°, 60° and 75° from the perpendicular to the tissue surface. The images demonstrate that the tissue has little polarization sensitivity when the incident light beam scans the tissue at the normal (0°) direction to the surface, but the degree of polarization sensitivity increases when the incident angle increases from the normal. The graphs of the phase retardation versus the depth for different incident angles of normal articular cartilage are shown in Fig. 8.

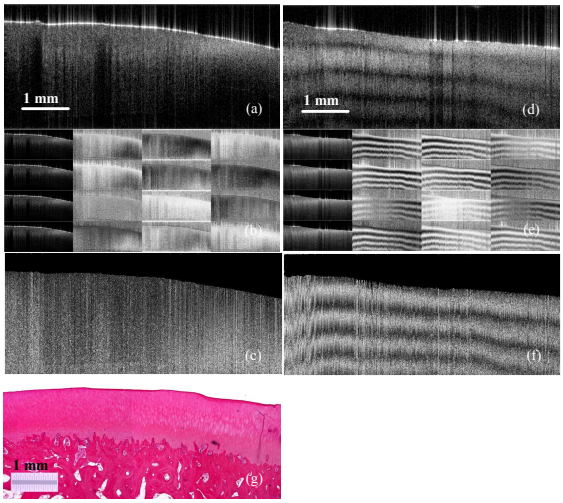

Fig. 5. OCT images ((a) and (d)) and Strokes vectors images ((b) and (e)) (6 mm×2.8 mm) and phase retardation images ((c) and (f)) and histology (g) when the incident light scanned a normal bovine articular cartilage specimen from the perpendicular to the articular surface (a, b, c) and along a cut plane made 90º to the articular surface (d, e, f).

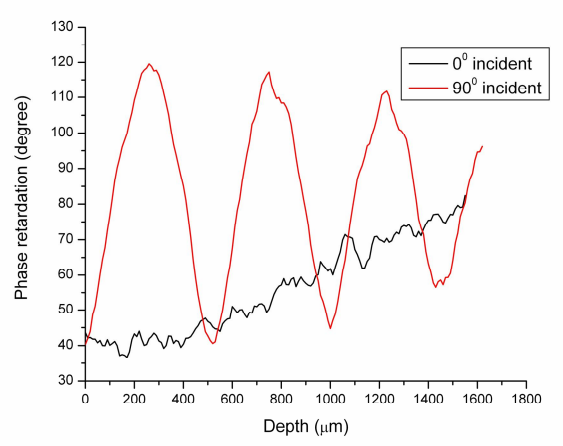

Fig. 6. Phase retardation versus depth when the incident light scanned a normal bovine articular cartilage specimen in a perpendicular (0°) and parallel (90º) direction relative to the specimen surface.

4. Discussion and Conclusion

The degree of birefringence (or polarization sensitivity) of articular cartilage is related to the orientlage and organization of the collagen fibrillar network of the cartilage matrix [21]. In the superficial zone of articular cartilage the collagen fibrils are oriented parallel to the surface, therefore, the accumulated retardation is expected to increase with depth in this region when the incident beam is perpendicular to the articular surface. As the incident beam travels into the deep zone, it is traveling parallel to the orientation of the collagen fibrils in this region and minimal to no phase retardation is expected. However, the deep zone demonstrates strong polarization sensitive when the incident light is directed along a

cut surface, perpendicular to the orientation of the collagen fibrils in a direction similar to the transillumination of histology sections viewed by polarization microscopy. The experimental results demonstrate that the degree of polarization sensitivity of normal articular cartilage increases as the incident light angle increases away from the perpendicular to the tissue surface. This directional sensitivity is related to the angle of incidence of the scanning beam relative to the orientation of the collagen fibrils and fibers of the cartilage and could be used to detect the spatial orientation pattern and organization of the collagen matrix of cartilage in health and disease.

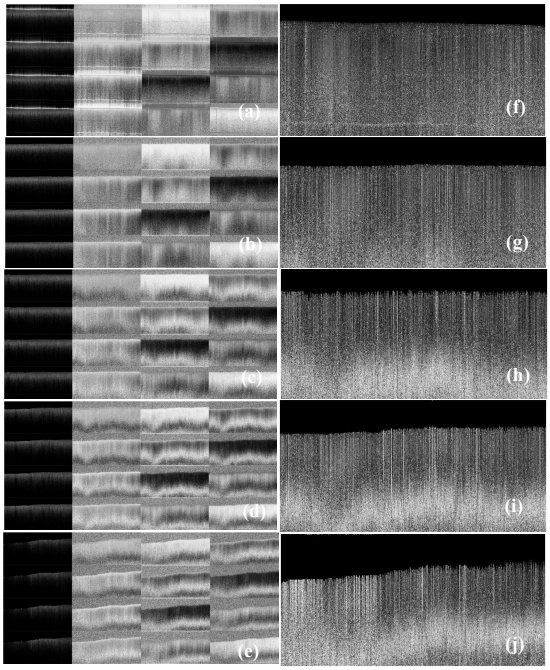

Fig. 7. Strokes vectors images (6 mm×2.8 mm) (a-d) and phase retardation images (f –j) of a normal articular cartilage when the incident light beam is 0^0 (a and f), 20^0 (b and g), 40^0 (c and h), 60^0 (d and i), and 75^0 (e and j) from the perpendicular to the articular surface.

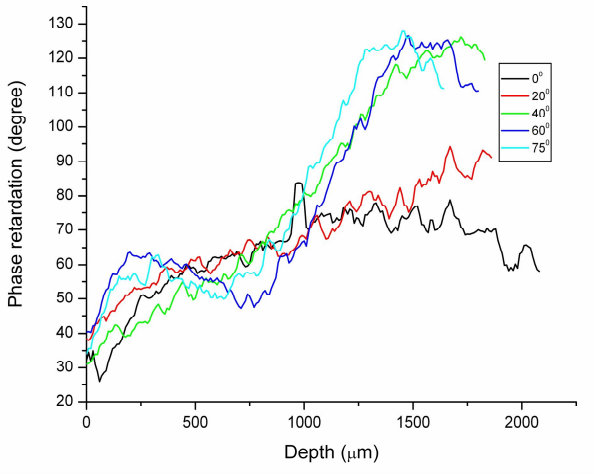

Fig. 8. Plot of phase retardation versus depth in a normal articular cartilage when the incident light beam is 0^0, 20^0, 40^0, 60^0, and 75^0 from the perpendicular the articular surface.

In summary, PS-OCT images can delineate the microstructure of articular cartilage and also provide information about their birefringence properties. They demonstrate that normal articular cartilage has little polarization sensitivity when the incident light beam scans the tissue at the perpendicular direction to the specimen surfaces. The degree of polarization sensitivity of normal articular cartilage when the light incident angle changes from 0º to 90º. These directional changes in polarization sensitivity are related to the incident angle of illumination relative to the orientation of collagen fibrils and fibers of the cartilage matrix and may be able to provide valuable information regarding the tissue matrix in healthy and diseased status.

Acknowledgement

We are pleased to acknowledge the assistance of Lih-huei Liaw, Paula Sweet and Sharon Evander in acquisition of specimens and histological processing. This work was supported by the U.S. Air Force Office of Scientific Research, Medical Free-Electron Laser Program (F49620-00-1-0371), the National Center for Research Resources of the National Institutes of Health (Laser Microbeam and Medical Program, RR-01192), the National Cancer Institute (CA-91717) and the Arnold and Mabel Beckman Foundation. The U.S. Government is authorized to reproduce and distribute reprints for Governmental purposes notwithstanding any copyright notation. The views and conclusions contained herein are those of the authors and should not be interpreted as necessarily representing the official policies or endorsements, either expressed or implied, of the Air Force Research Laboratory or the U.S. Government.

References

1. Osteoarthritis, US National Institute of Health, National institute of Arthritis and Musculoskeletal and Skin Diseases (2002).
2. W. P. Chan, P. Lang, M. P. Stevens, K. Sack, S. Majumdar, D. W. Stroller, et al., "Osteoarthritis of the knee: comparison of radiography, CT, and MR imaging to assess extent and severity," Am J Roentgenol, **157**, 799-806 (1991).
3. K. P. Speer, C. E. Spritzer, J. L. Goldner, W. E. Jr. Garrett, "Magnetic resonance imaging of traumatic knee articular cartilage injuries," Am J Sports Med, **9**, 396-402 (1991).
4. J. A. Tyler, P. J. Watson, K. Hwee-Ling, et al., "Detection and monitoring of progressive degeneration of osteoarthritic cartilage by MRI," Acta Orthop Scand; **66 Suppl 2**, 130-138 (1995).
5. S. L. Myers, K. Dines, D. A. Brandt, K. D. Brandt, M. E. Albrecht, "Experimental assessment by high frequency ultrasound of articular cartilage thickness and osteoarthritic changes," J Rheumatol., **22**, 109-116 (1995).
6. A. D. Aguirre, P. Hsiung, T. H. Ko, I. Hartl, J. G. Fujimoto, "High-resolution optical coherence microscopy for high-speed, in vivo cellular imaging," Optics Letters, **28**, 2064-2066 (2003).
7. Y. Pan, Z. Li, T. Xie, C. R. Chu, "Hand-held arthroscopic optical coherence tomography for in-vivo high-resolution imaging of articular cartilage," J Biomedical Optics, **8(4),** 648-654 (2003).
8. J. F. de Boer, T. E. Milner, M. J. C. van Gemert, and J. S. Nelson, "Two-dimensional birefringence imaging in biological tissue by polarization-sensitive optical coherence tomography," Opt. Lett. **22**, 934-936 (1997).
9. S. Jiao, L. Wang, "Jones Matrix imaging of biological tissues with quadruple-channel optical coherence tomography," J Biomed. Opt., **7 (3)**, 350-358 (2002).
10. C. E. Saxer, J. F. De Boer, B. H. Park, Y. Zhao, Z. Chen, and J. S. Nelson, "High-speed fiber-based polarization-sensitive optical coherence tomography of in vivo human skin," Opt. Lett., **25**, 1355-1357 (2000).
11. W. Drexler, D. Stamper, C. Jesser, X. Li, C. Pitris, K. Saunders, S. Martin, M. B. Lodge, J. G. Fujimoto, and M. E. Brezinski, "Correlation of collagen organization with polarization sensitive imaging of in vitro cartilage: implications for osteoarthritis," J. Rheumatol., **28,** 1311-1318 (2001).
12. Tuqiang Xie, Shuguang Guo, Jun Zhang, Zhongping Chen, George M. Peavy, "Determination of characteristics of degenerative joint disease using optical coherence tomography and polarization sensitive optical coherence tomography," submitted (2005).
13. S. J. Matcher, C. P. Winlove, S. V. Gangnus, "The collagen structure of bovine intervertebral disc studied using polarization-sensitive optical coherence tomography," Phys. Med. & Bio., **49,** 1295-1306 (2004).
14. J. M. Herman, C. Pitris, B. E. Bouma, S. A. Boppart, C. A. Jesser, D. L. Stamper, J. G. Fujimoto, and M. E. Brezinski, "High resolution imaging of normal and osteoarthritic cartilage with optical coherence tomography," J. Rheumatol., **26,** 627-635 (1999).

15. J. Zhang, S. Guo, W. Jung, J. S. Nelson, and Z. Chen, "Determination of birefringence and absolute optic axis orientation using polarization-sensitive optical coherence tomography with PM fibers," Optics Express, **11,** 3262-70 (2003).
16. B. H. Park, C. Saxer, S. M. Sringivas, J. S. Nelson, and J. F. de Boer, "In vivo burn depth determination by high-speed fiber-based polarization sensitive optical coherence tomography," J Biomedical Optics; **6**, 474-479 (2002).
17. M. A. MacConiall, "The movements of bones and joints: 4. the mechanical structure of articulating cartilage," J Bone Joint Surg Br, **33B**, 251-257 (1951).
18. C. Weiss, L. Rosenberg, A. J. Helfet, "An ultrastructural study of normal young adult human articular cartilage," J Bone Joint Surg AM, **50,** 663-674 (1968).
19. J. M. Clark, "The organization of collagen in cryofractured rabbit articular cartilage: a scanning electron microscopic study," Journal of Orthopaedic Research, **3,** 17-29 (1985).
20. J. Dunham, D. R. Shackleton, M. E. J. Billingham, L. Bitensky, J. Chayen, H. Muir, "A reappraisal of the structure of normal canine articular cartilage," J Anat., **157,** 89-99 (1988).
21. K. Kiraly, M. M. Hyttinen, T. Lapvetelainen, M. Elo, I. Kiviranta, J. Dobai, L. Modis, H. J. Helminen and J. P. A. Arokoski, "Specimen preparation and quantification of collagen birefringence in unstained sections of articular cartilage using image analysis and polarizing light microscopy," Histochemical Journal, **29,** 317-327 (1997).